Journal of Southeast University (English Edition) Vol. 23, No. 4, pp. 479 - 483 Dec. 2007 ISSN 1003—7985

Close-formed bound on generalized distributed antenna system capacity

Sun Huan Wang Xinyu You Xiaohu

(National Mobile Communications Research Laboratory, Southeast University, Nanjing 210096, China)

Abstract: The composite channel models of the generalized distributed antenna system (GDAS) such as Rayleigh-lognormal fading are studied. Then comparisons are performed between the GDAS and the traditional multiple-input multiple-output (MIMO) system to analyze the ergodic capacity of the GDAS and make conclusions that it is impossible to achieve an analytical expression for the ergodic capacity of the GDAS. Moreover, in order to evaluate the performance of the ergodic capacity of the GDAS conveniently, the analytical lower bound and upper bound of the ergodic capacity of the GDAS are derived by using the results from multivariate statistics and matrix inequalities, under the scenarios of Rayleigh-lognormal fading and equal power allocation scheme at transmitter. Finally, the analytical bounds are verified by comparisons with the numerical results.

Key words: generalized distributed antenna system; ergodic capacity; multiple-input multiple-output; Rayleigh-lognormal fading

Future wireless systems will need to provide high data rates and high quality service. One promising technique, the distributed antenna system (DAS), is refocused recently for its many merits, such as larger coverage area, longer battery life of terminal and higher system capacity, etc. In the DAS, antenna modules are geographically distributed and each distributed antenna module is connected to the same central processing unit through coaxial cable or fiber. In addition, a distributed antenna module is called a port when it is equipped with many antennas, and the DAS is extended to a generalized DAS (GDAS). The DAS was originally used to cover the dead spots in indoor wireless communication[1]. Recently, the outage capacity of the GDAS has been investigated in Ref. [2] whose outage performance outperforms that of the traditional multiple input multiple output (MIMO) system (In some existing works, the traditional MIMO is also called standard cell MIMO). The capacity of the GDAS has been demonstrated only in numerical simulation[3] for its high complexity probability density function (PDF) of the GDAS channel matrix, whose entry involves both macro fading and micro fading. Han et al. [4] researched the upper bounds of G-DWCS capacity in which the GDAS was adopted by the DWCS which was first given by Zhou et al. [5], but all of their analyses and simulations neglected the shadowing effect on capacity performance.

The channel model of the traditional MIMO system is simpler than that of the GDAS, but the expression of its average capacity formula is very complex which causes much difficulty in evaluating MIMO system capacity performance. Thus, we can predict that the expression of the average capacity of the GDAS concerns more complex structures than that of the traditional MIMO system. In order to effectively evaluate the capacity performance of the GDAS, we utilize the multivariate theories and matrix inequality results to perform the analysis. This paper achieves both upper and lower bounds of the average capacity of a generalized distributed antenna system, which contains components of the macro-fading and the micro-fading that affects system capacity performance. Numerical simulations demonstrate the validity of the analytical results in evaluating the performance of capacity.

1 System Model

In this paper, we take the same system model as that adopted in Ref. [4], which is denoted by (N/K, K, M), where M, N and K represent the number of receiver antennas, the total number of transmit antennas and the port numbers, respectively. All the N/K antennas in one port are connected to a central processing unit through coaxial cable or fiber and those signals are processed simultaneously in this unit. Due to the geographically distribution among the ports, the macroscopic fading

Received 2007-05-16.

Foundation item: The National Natural Science Foundation of China (No. 60496311).

Biographies: Sun Huan (1974—), male, graduate; You Xiaohu (corresponding author), male, doctor, professor, xhyu@seu.edu.cn.

(pass loss and shadowing) between different ports are generally independent. Microscopic fading of each antenna within one port is assumed as Rayleigh fading. The distance between a mobile terminal and each port is denoted as $d_1, d_2, \ldots, d_K$, a received signal can be expressed as[4]

$$\boldsymbol{y} = \boldsymbol{H}\boldsymbol{x} + z = \boldsymbol{H}_w\boldsymbol{T}\boldsymbol{x} + z \tag{1}$$

where $\boldsymbol{y}$ and $\boldsymbol{x}$ denote the received and transmitted vectors, respectively; z presents a noise vector with i. i. d $CN(0, 1)$ entries; $\boldsymbol{H}$ is the channel matrix; large scale fading can be denoted by a local stationary $N \times N$ diagonal matrix $\boldsymbol{T} = \text{diag}(\sqrt{\alpha_1} \ldots, \sqrt{\alpha_1}, \ldots, \sqrt{\alpha_K}, \ldots, \sqrt{\alpha_K})$ and small-scale fading is modeled as Rayleigh fading denoted by an $M \times N$ matrix $\boldsymbol{H}_w$ with i. i. d $CN(0, 1)$ entries. The diagonal entries of $\boldsymbol{T}$ are modeled both shadowing and path loss, i. e. $\alpha_k = cs_k/d_k^{\gamma}$, where the shadowing is represented by a log-normal random variable s_j, and γ is the path loss exponent which varies from 2 to 6 depending on the terrain and foliage. Several empirically based path loss models have been developed for macro-cellular and micro-cellular environments, such as the Okumura, Hata, COST-231 and Erceg models. For simplicity of exposition here, the constant c is set to 1. So α_k is still a log-normal variable and its PDF can be expressed as

$$f(\alpha_k) = \frac{\xi}{\sqrt{2\pi}\alpha_k\sigma_k}\exp\left[-\frac{(\xi\ln\alpha_k - \mu_k)^2}{2\sigma_k^2}\right] \tag{2}$$

where $\mu_k = E[10\log_{10}\alpha_k]$, $\sigma_k^2 = \text{var}(10\log_{10}\alpha_k)$, $\xi = 10/\ln 10$. In the next section, this channel model is used to investigate the system capacity performance and to study the effects of macro and micro fading on it.

2 Capacity Bound Analysis

As assumed in section 1, channel state information is not available at the transmitter but fully available at the receiver. The transmitting power is equally allocated among ports and antennas in each port. From the receiving model in Eq. (1), the downlink capacity of the GDAS for a specific port distribution and channel realization is expressed as

$$C = \ln\left|\boldsymbol{I} + \frac{\rho}{N}(\boldsymbol{H}_w\boldsymbol{T})(\boldsymbol{H}_w\boldsymbol{T})^{\mathrm{H}}\right| = \ln\left|\boldsymbol{I} + \frac{\rho}{N}\boldsymbol{H}_w\boldsymbol{T}^2\boldsymbol{H}_w^{\mathrm{H}}\right| \tag{3}$$

where $|\cdot|$ denotes the determinant of a matrix, and ρ is the transmitting power to receive noise variance ratios. It is shown in Eq. (3) that the instant capacity is a variable, so the average capacity is required to be calculated to evaluate its performance. Also in Eq. (3), the role of matrix $\boldsymbol{T}$ is similar to the transmit covariance matrix in the spatial correlated MIMO channel even if we only consider the path loss. But many existing results of a spatially correlated MIMO channel cannot be directly applied to Eq. (3) because it requires distinct eigenvalues of the transmitting covariance matrix[6]. However, matrix $\boldsymbol{T}$ has some identical eiguenvalues which are defined by the special structure of the GDAS.

As a special case in our study, when the research of the capacity performance of the GDAS only considers the pass loss effect, we use different methods for different system structures. For example, concerning a GDAS system with the special structure $(1, N, 1)$, the average capacity can be approximately achieved by Pearson's approach[7].

When the number of receiver antennas is greater than one, we can use the method of the moment generating function to evaluate capacity performance. In a given mobile position of GDAS, $\boldsymbol{T}$ is a constant matrix and it has some identical diagonal entries. Under this condition, the average capacity can be calculated by the following steps. First, we assume that all diagonal entries are distinct and then calculate the moment function of $\boldsymbol{H}_w\boldsymbol{T}^2\boldsymbol{H}_w^{\mathrm{H}}$. After that, work out the derivative of moment function for the related variable and take the limits of corresponding variable to the actual value later. Finally, using the relationship between average capacity and its moment function, the analytic expression of average capacity can be achieved. The detailed procedure of this method can be found in Ref. [8]. But the derivative operation makes the expression of capacity more complex due to its involving the matrix derivation.

However, when both the pass loss and shadowing are considered, the above mentioned method is invalidated. For evaluating the capacity performance effectively and completely, the average capacity bound is studied and used to indicate the actual capacity performance.

In the following, close-formed lower bounds and upper bounds of the average capacity of the generalized distributed antennas system are derived. The bounds contain effects of macro-fading and micro-fading on the average capacity of the system. In brief, during the deduction, we let matrix $\boldsymbol{F} = \boldsymbol{T}^2$. $\boldsymbol{W} = \boldsymbol{H}_w\boldsymbol{H}_w^{\mathrm{H}}$, $M \leqslant N$ or $\boldsymbol{W} = \boldsymbol{H}_w^{\mathrm{H}}\boldsymbol{H}_w$, $M > N$, where $\boldsymbol{W}$ is a Wishart matrix. The lower bounds of average capacity are thus first derived.

2.1 Lower bound analysis

In this subsection, the lower bounds of the average

capacity of the GDAS are derived. In the following deductions, this topic is divided into two cases to be analyzed according to different antenna configurations at the transmitter and the receiver.

Case 1 $N \leqslant M$. The number of transmitter antennas is less than or equal to the number of receiver antennas. From Eq. (3), we can obtain

$$C = \ln\left|\boldsymbol{I}_M + \frac{\rho}{N}\boldsymbol{H}_{\mathrm{w}}\boldsymbol{F}\boldsymbol{H}_{\mathrm{w}}^{\mathrm{H}}\right| = \ln\left|\boldsymbol{I}_N + \frac{\rho}{N}\boldsymbol{F}\boldsymbol{H}_{\mathrm{w}}^{\mathrm{H}}\boldsymbol{H}_{\mathrm{w}}\right| =$$
$$\ln\prod_{i=1}^{N}\left(1+\lambda_i\left(\frac{\rho}{N}\boldsymbol{F}\boldsymbol{H}_{\mathrm{w}}^{\mathrm{H}}\boldsymbol{H}_{\mathrm{w}}\right)\right) \geqslant$$
$$\ln\left(1+\frac{\rho}{N}|\boldsymbol{F}\boldsymbol{H}_{\mathrm{w}}^{\mathrm{H}}\boldsymbol{H}_{\mathrm{w}}|^{\frac{1}{N}}\right)^N =$$
$$N\ln\left(1+\frac{\rho}{N}\exp\frac{1}{N}\ln(|\boldsymbol{F}||\boldsymbol{H}_{\mathrm{w}}^{\mathrm{H}}\boldsymbol{H}_{\mathrm{w}}|)\right) =$$
$$N\ln\left(1+\frac{\rho}{N}\exp\frac{1}{N}(\ln|\boldsymbol{F}|+\ln|\boldsymbol{H}_{\mathrm{w}}^{\mathrm{H}}\boldsymbol{H}_{\mathrm{w}}|)\right) \quad (4)$$

The inequality in Eq. (4) uses the facts: $\prod_{j=1}^{N}(1+x_j) \geqslant (1+x_{\mathrm{gm}})^N$, where $x_j > 0, x_{\mathrm{gm}} = \left(\prod_{j=1}^{N}x_j\right)^{\frac{1}{N}}$. At the same time, due to $\log(1+\alpha\exp(x)), \alpha > 0$ is a convex function of x. The lower bound can be achieved as

$$E(C) \geqslant N\ln\left(1+\frac{\rho}{N}\exp\frac{1}{N}(E\ln|\boldsymbol{F}|+E\ln|\boldsymbol{H}_{\mathrm{w}}^{\mathrm{H}}\boldsymbol{H}_{\mathrm{w}}|)\right) =$$
$$N\ln\left(1+\frac{\rho}{N}\exp\frac{1}{N}\left(\sum_{i=1}^{N}h\mu_i+\sum_{i=0}^{N-1}\psi(M-i)\right)\right) \quad (5)$$

where $\psi(\cdot)$ is Euler's digamma function[9]. For natural arguments it can be expressed as $\psi(n) = \psi(n-1) + \frac{1}{n-1}$, with $-\psi(1) = 0.577\,215\ldots$ the Euler-Mascheroni constant.

Case 2 $N > M$. The number of transmitters is greater than that of the receiver antennas. Here we only consider the constraint on the relationship between the number of transmit antennas and that of the receiver on $2M \geqslant N > M$. If $N > 2M$, the lower bound can be derived via the same method. Under this constraint, channel matrix $\boldsymbol{H}_{\mathrm{w}}$ can be rewritten into block matrices as $\boldsymbol{H}_{\mathrm{w}} = [\boldsymbol{H}_{\mathrm{w1}}, \boldsymbol{H}_{\mathrm{w2}}]$, where $\boldsymbol{H}_{\mathrm{w1}}$ is an $M \times M$ matrix and $\boldsymbol{H}_{\mathrm{w2}}$ is an $M \times (N-M)$ matrix. So $\boldsymbol{H}_{\mathrm{w1}}\boldsymbol{H}_{\mathrm{w1}}^{\mathrm{H}} \sim W_M(M, \boldsymbol{I})$ and $\boldsymbol{H}_{\mathrm{w2}}^{\mathrm{H}}\boldsymbol{H}_{\mathrm{w2}} \sim W_{N-M}(M, \boldsymbol{I})$, where $W_n(m, \boldsymbol{I})$ denotes the central complex Wishart distribution. Also, the diagonal matrix $\boldsymbol{F}$ can be rewritten in block matrix as $\boldsymbol{F} = \mathrm{diag}(\boldsymbol{F}_1, \boldsymbol{F}_2)$, where $\boldsymbol{F}_1$ is an $M \times M$ diagonal matrix, whose diagonal entry is the same as that of $\boldsymbol{F}$ in the same order, $\boldsymbol{F}_2$ is an $(N-M) \times (N-M)$ diagonal matrix. Its diagonal entry is the same as that of the last $(N-M)$ entry of $\boldsymbol{F}$ in the same order. Then the average capacity lower bound can be expressed as

$$E(C) = E\left(\ln\left|\boldsymbol{I}_M + \frac{\rho}{N}\boldsymbol{H}_{\mathrm{w}}\boldsymbol{F}\boldsymbol{H}_{\mathrm{w}}^{\mathrm{H}}\right|\right) =$$
$$E\left(\ln\left|\frac{1}{2}\left(\boldsymbol{I}_M+\boldsymbol{I}_M+\frac{2\rho}{N}\boldsymbol{H}_{\mathrm{w}}\boldsymbol{F}\boldsymbol{H}_{\mathrm{w}}^{\mathrm{H}}\right)\right|\right) \geqslant$$
$$\frac{1}{2}E\left(\ln\left|\boldsymbol{I}_M+\frac{2\rho}{N}\boldsymbol{H}_{\mathrm{w1}}\boldsymbol{F}_1\boldsymbol{H}_{\mathrm{w1}}^{\mathrm{H}}\right|\right) +$$
$$\frac{1}{2}E\left(\ln\left|\boldsymbol{I}_M+\frac{2\rho}{N}\boldsymbol{H}_{\mathrm{w2}}\boldsymbol{F}_2\boldsymbol{H}_{\mathrm{w2}}^{\mathrm{H}}\right|\right) \geqslant$$
$$\frac{1}{2}M\ln\left(1+\frac{2\rho}{N}\exp\frac{1}{M}\left(\sum_{i=1}^{M}h\mu_i+\sum_{i=0}^{M-1}\psi(M-i)\right)\right) +$$
$$\frac{1}{2}(N-M)\ln\left(1+\frac{2\rho}{N}\exp\frac{1}{N-M}\left(\sum_{i=1}^{N-M}h\mu_i+\sum_{i=0}^{N-M-1}\psi(M-i)\right)\right) \quad (6)$$

The first inequality in formula (6) results from the Ky Fan inequality[10]. If $\boldsymbol{A}, \boldsymbol{B}$ are positive definite matrices, ($\boldsymbol{A} > 0$ and $\boldsymbol{B} > 0$), then, $\ln\det(\alpha\boldsymbol{A} + (1-\alpha)\boldsymbol{B}) \geqslant \alpha\ln\det\boldsymbol{A} + (1-\alpha)\ln\det\boldsymbol{B}$. And the second inequality in formula (6) uses the result of case 1. So far, the lower bounds of the average capacity of the GDAS are derived.

2.2 Upper bound analysis

In this subsection, the upper bounds of the average capacity of the GDAS are derived. The deduction is also divided into two cases to be discussed according to antenna configurations at the transceiver.

Case 1 $N \leqslant M$. The number of transmitter antennas is less than or equal to the number of receiver antennas. Under this condition, we can obtain

$$E(C) = E\left(\ln\left|\boldsymbol{I}_M + \frac{\rho}{N}\boldsymbol{H}_{\mathrm{w}}\boldsymbol{F}\boldsymbol{H}_{\mathrm{w}}^{\mathrm{H}}\right|\right) =$$
$$E\left(\ln\left|\boldsymbol{I}_N + \frac{\rho}{N}\boldsymbol{F}\boldsymbol{H}_{\mathrm{w}}^{\mathrm{H}}\boldsymbol{H}_{\mathrm{w}}\right|\right) \leqslant$$
$$E\left(\ln\prod_{i=1}^{N}\left(1+\frac{\rho}{N}[\boldsymbol{F}]_{i,i}[\boldsymbol{W}]_{i,i}\right)\right) \leqslant$$
$$\sum_{i=1}^{N}\ln\left(1+\frac{\rho}{N}E([\boldsymbol{F}]_{i,i})E([\boldsymbol{W}]_{i,i})\right) =$$
$$\sum_{i=1}^{N}\ln\left(1+\frac{\rho}{N}\exp\left(h\mu_i+\frac{(h\sigma_i)^2}{2}\right)M\right) =$$
$$\sum_{i=1}^{N}\ln\left(1+\frac{\rho M}{N}\exp\left(h\mu_i+\frac{(h\sigma_i)^2}{2}\right)\right) \quad (7)$$

where $[\boldsymbol{W}]_{i,j}$ presents the (i,j)-th element of matrix $\boldsymbol{W}$. The first inequality in (7) follows from the Hadamard inequality[11], and the second inequality in (7) results from the Jensen inequality[11].

Case 2 $N > M$. The number of transmitters is greater than that of the receiver antennas. The capacity C can be rewritten as

$$C = \ln\left|\boldsymbol{I}_M + \frac{\rho}{N}\boldsymbol{H}_w\boldsymbol{F}\boldsymbol{H}_w^H\right| \leqslant \ln\left|\boldsymbol{I}_M + \frac{\rho \mathrm{tr}(\boldsymbol{F})}{N^2}\boldsymbol{H}_w\boldsymbol{H}_w^H\right| =$$

$$\ln\prod_{i=1}^{M}\left(1+\lambda_i\left(\frac{\rho \mathrm{tr}(\boldsymbol{F})}{N^2}\boldsymbol{H}_w\boldsymbol{H}_w^H\right)\right) \leqslant \ln\left(\frac{\sum_{i=1}^{M}(1+\lambda_i)}{M}\right)^M =$$

$$M\ln\left(1+\frac{\rho}{MN^2}\mathrm{tr}(\boldsymbol{F})\mathrm{tr}(\boldsymbol{H}_w\boldsymbol{H}_w^H)\right) \quad (8)$$

where $\mathrm{tr}(\boldsymbol{F})$ is the trace operation of matrix $\boldsymbol{F}$. The first inequality in (8) can be found in Ref. [12], and the second inequality in (8) results from arithmetical means and geometric means inequalities. So the upper bound of average capacity can be expressed as

$$E(C) \leqslant M\ln\left(1+\frac{\rho}{MN^2}E\mathrm{tr}(\boldsymbol{F})E\mathrm{tr}(\boldsymbol{H}_w\boldsymbol{H}_w^H)\right) =$$

$$M\ln\left(1+\frac{\rho}{MN^2}\sum_{i=1}^{N}\exp\left(h\mu_i+\frac{(h\sigma_i)^2}{2}\right)MN\right) =$$

$$M\ln\left(1+\frac{\rho}{N}\sum_{i=1}^{N}\exp\left(h\mu_i+\frac{(h\sigma_i)^2}{2}\right)\right) \quad (9)$$

3 Simulation and Discussion

In this section, the comparisons between the numerical simulations and the analytical lower and upper bounds of the average capacity of the GDAS are performed. In all simulations, it is assumed that all the different sub-channels undergo the same shadowing with the same standard deviation σ, and the pass loss exponent γ is set at 2.5. Considering a square region with one antenna at each vertex, the area is L^2 and the mobile with four receive antennas is randomly located inside.

First, the numerical simulation of the average capacity in this region is presented in Fig. 1 with $\rho = 30$ dB, $\sigma = 6$ dB and $L = 20$ m.

As shown in Fig. 1, the user location has an important effect on the system capacity. Also it can be seen that the lowest capacity is achieved when the user is located in the center point of the concerned region.

Simulations of the average capacity of one fixed position and the average capacity of the concerned region area are performed to demonstrate that the bounds are able to describe the capacity of the GDAS correctly. Comparisons between the simulation results and the analytical bounds are illustrated in Fig. 2 and Fig. 3, respectively.

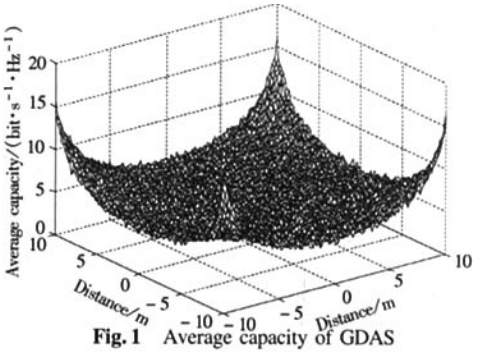

Fig. 1 Average capacity of GDAS

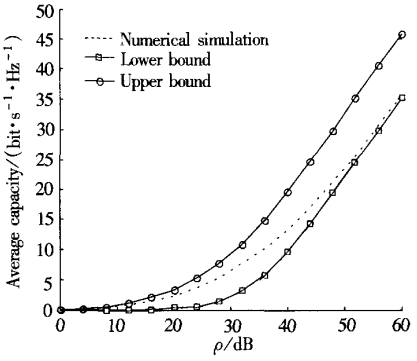

Fig. 2 Average capacity and bounds on the central position ($\gamma = 2.5$, $\sigma = 6$ dB)

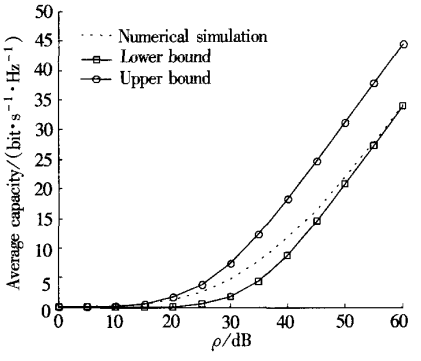

Fig. 3 Average capacity and bounds on the concerned region area ($\gamma = 2.5$, $\sigma = 6$ dB, $L = 20$ m)

In Fig. 2, it is assumed that the user is located in the centre of the researching region. From the plot, it can be seen that at the low ρ region, the average capacity is well approximated by the upper bound, while at the high ρ region, the lower bound performance is better than that of the upper bound. In Fig. 3, it is assumed that the user's position is a random variable with unique distribution in the region being researched. The average capacity of the area is calculated. From the comparison between the numerical simulation result and the analytical bounds, it can be concluded that those bounds can be well used to evaluate the system capacity of the GDAS effectively.

4 Conclusion

The analytical expression of the erogidc capacity of the GDAS is still an open problem. In this paper, we utilize multivariate theories and matrix inequality theories to analyze the ergodic capacity of the GDAS and

derive its lower bounds and upper bounds. Simulation results demonstrate that those analytical bounds can be used to characterize the performance of the ergodic capacity of the GDAS. Furthermore, based on these results, the technique of transmit antenna selection and the adaptive transmissions of the GDAS are investigated.

References

[1] Saleh A A M, Rustako A J, Roman R S. Distributed antennas for indoor radio communications [J]. *IEEE Trans Commun*, 1987, **35**(12): 1245 - 1251.

[2] Roh Wonil, Paulraj A. Outage performance of the distributed antenna systems in a composite fading channel [C]// *Proceedings of VTC* 2002-*Fall*. Vancouver, BC, Canada, 2002: 1520 - 1524.

[3] Roh Wonil. High performance distributed antenna cellular network[D]. Stanford University, 2003.

[4] Han Shuangfeng, Zhou Shidong, Wang Jing. Downlink capacity analysis and transmit antenna selection of generalized distributed wireless communication system [C]//*Proceedings of VTC* 2004-*Fall*. Los Angeles, 2004: 2186 - 2190.

[5] Zhou Shidong, Zhao Ming, Xu Xibin, et al. Distributed wireless communication system: a new architecture for future public wireless access[J]. *IEEE Commun Mag*, 2003, **41**(3): 108 - 113.

[6] Tulino A M, Verdu S. Random matrix theory and wireless communications[J]. *Foundations and Trends in Commun and Inf Theory*, 2004, **1**(1): 1 - 182.

[7] Mathai A M. *Quadratic forms in random variables: theory and application*[M]. New York: Dekker, 1992.

[8] Simon S H, Moustakas A L, Marinelli L. Capacity and character expansions: moment-generating function and other exact results for MIMO correlated channels[J]. *IEEE Trans Inform Theory*, 2006, **52**(12): 5336 - 5351.

[9] Gradshteyn S, Ryzhik I. *Table of integrals, series and products*[M]. New York: Academic Press, 1965.

[10] Wang Songgui, Wu Mixia. *Matrix inequality*[M]. 2nd ed. Beijing: Science Press, 2006. (in Chinese)

[11] Cover T M, Thomas J A. *Elements of information theory* [M]. John Wiley and Sons, Inc, 1991.

[12] Telatar I E. Capacity of multi-antenna Gaussian channels [J]. *European Trans Telecommunication*, 1999, **10**(6): 585 - 596.

广义分布式天线系统容量解析界

孙 欢 王新宇 尤肖虎

(东南大学移动通信国家重点实验室,南京 210096)

摘要:首先对广义分布式天线系统的复合信道模型,如瑞利对数正态衰落信道模型,进行了分析.通过与传统多输入多输出系统的比较,对广义分布式天线系统容量进行了分析,并得出广义分布式天线系统历经容量完整的解析表达式是不可能存在的.为了有效地对广义分布式天线系统历经容量的性能进行评估,利用多元统计理论和矩阵不等式理论推导了在瑞利对数正态衰落信道模型及在发射端采用等功率分配方案下广义分布式天线系统历经容量的解析下界和解析上界.最后,通过数值仿真证明了系统的历经容量可以很好地用其解析界来表述.

关键词:广义分布式天线系统;历经容量;多输入多输出;瑞利对数正态衰落

中图分类号:TN929.5

如 何 学 习 天 线 设 计

天线设计理论晦涩高深，让许多工程师望而却步，然而实际工程或实际工作中在设计天线时却很少用到这些高深晦涩的理论。实际上，我们只需要懂得最基本的天线和射频基础知识，借助于 HFSS、CST 软件或者测试仪器就可以设计出工作性能良好的各类天线。

易迪拓培训(www.edatop.com)专注于微波射频和天线设计人才的培养，推出了一系列天线设计培训视频课程。我们的视频培训课程，化繁为简，直观易学，可以帮助您快速学习掌握天线设计的真谛，让天线设计不再难…

HFSS 天线设计培训课程套装

套装包含 6 门视频课程和 1 本图书，课程从基础讲起，内容由浅入深，理论介绍和实际操作讲解相结合，全面系统的讲解了 HFSS 天线设计的全过程。是国内最全面、最专业的 HFSS 天线设计课程，可以帮助你快速学习掌握如何使用 HFSS 软件进行天线设计，让天线设计不再难…

课程网址：http://www.edatop.com/peixun/hfss/122.html

CST 天线设计视频培训课程套装

套装包含 5 门视频培训课程，由经验丰富的专家授课，旨在帮助您从零开始，全面系统地学习掌握 CST 微波工作室的功能应用和使用 CST 微波工作室进行天线设计实际过程和具体操作。视频课程，边操作边讲解，直观易学；购买套装同时赠送 3 个月在线答疑，帮您解答学习中遇到的问题，让您学习无忧。

详情浏览：http://www.edatop.com/peixun/cst/127.html

13.56MHz NFC/RFID 线圈天线设计培训课程套装

套装包含 4 门视频培训课程，培训将 13.56MHz 线圈天线设计原理和仿真设计实践相结合，全面系统地讲解了 13.56MHz 线圈天线的工作原理、设计方法、设计考量以及使用 HFSS 和 CST 仿真分析线圈天线的具体操作，同时还介绍了 13.56MHz 线圈天线匹配电路的设计和调试。通过该套课程的学习，可以帮助您快速学习掌握 13.56MHz 线圈天线及其匹配电路的原理、设计和调试…

详情浏览：http://www.edatop.com/peixun/antenna/116.html

关于易迪拓培训：

易迪拓培训(www.edatop.com)由数名来自于研发第一线的资深工程师发起成立，一直致力和专注于微波、射频、天线设计研发人才的培养；后于 2006 年整合合并微波 EDA 网(www.mweda.com)，现已发展成为国内最大的微波射频和天线设计人才培养基地，成功推出多套微波射频以及天线设计经典培训课程和 ADS、HFSS 等专业软件使用培训课程，广受客户好评；并先后与人民邮电出版社、电子工业出版社合作出版了多本专业图书，帮助数万名工程师提升了专业技术能力。客户遍布中兴通讯、研通高频、埃威航电、国人通信等多家国内知名公司，以及台湾工业技术研究院、永业科技、全一电子等多家台湾地区企业。

我们的课程优势：

※ 成立于 2004 年，10 多年丰富的行业经验

※ 一直专注于微波射频和天线设计工程师的培养，更了解该行业对人才的要求

※ 视频课程、既能达到了现场培训的效果，又能免除您舟车劳顿的辛苦，学习工作两不误

※ 经验丰富的一线资深工程师主讲，结合实际工程案例，直观、实用、易学

联系我们：

※ 易迪拓培训官网：http://www.edatop.com

※ 微波 EDA 网：http://www.mweda.com

※ 官方淘宝店：http://shop36920890.taobao.com